

Time Domain Inverse Problem of a Buried Dielectric Cylinder

Chien-Ching Chiu, Ching-Lieh Li, Chung-Hsin Huang and Wan Ling Chang

Electrical Engineering Department, Tamkang University

Tamsui, Taiwan, R.O.C.

chiu@ee.tku.edu.tw

li@ee.tku.edu.tw

691350010@s91.tku.edu.tw

ling9_24@hotmail.com

Abstract—This paper presents an image reconstruction approach based on the time-domain and particle swarm optimization (PSO) for a 2-D homogeneous dielectric cylinder buried in a half-space. The computational method combines the finite difference time domain (FDTD) method and the particle swarm optimization (PSO) to determine the shape and location of the underground scatterer with arbitrary cross section. The subgridding technique is implemented in the FDTD code for modeling the shape of the cylinder more closely. In order to describe an unknown cylinder with arbitrary shape more effectively, the shape function is expanded by closed cubic-spline function instead of frequently used trigonometric series. The inverse problem is resolved by an optimization approach, and the global searching scheme PSO is then employed to searching the parameter space. In order to reduce the number of the unknown parameters for the inverse scattering, the shape function of the cylinder is interpolated in terms of the closed cubic-spline. Numerical results demonstrate that, even when the initial guess is far away from the exact one, good reconstruction can be obtained.

I. INTRODUCTION

The objective of the inverse scattering is to determine the electromagnetic properties of the scatterer from scattering field measured outside. Inverse scattering problems have attracted much attention in the past few years. This kind of problem has several important applications such as medical imaging, microwave remote sensing, geophysical exploration, and nondestructive testing. Traditional iterative inverse algorithms are founded on a functional minimization via some gradient-type scheme [1]. In general, during the search of the global minimum, they tend to get trapped in local minima when the initial guess is far from the exact one. Some global optimal searching method such as genetic algorithm [2], neural network [3], have be proposed to search the global extreme of the nonlinear functional problem. In the 1995, the J. Kennedy and R. Eberhart first proposed the particle swarm optimization (PSO) [4]. The particle swarm optimization is a population based stochastic optimization algorithm. It is a kind of swarm intelligence that is based on social behavior. This paper presents a computational scheme combining the FDTD and PSO to reconstruct the microwave imaging of a 2D homogeneous dielectric cylinder with arbitrary shape in free space. The forward problem is solved based on the FDTD

method, for which the subgridding technique is implemented to closely describe the fine structure of the cylinder [5]. The inverse problem is formulated into an optimization one and then the global searching scheme PSO is used to searching the parameter space. Interpolation technique through the cubic spline is employed to reduce the number of parameters needed to closely describe a cylinder of arbitrary shape as compared to the Fourier series expansion

II. SUBGRID FDTD

Consider a 2-D homogeneous dielectric cylinder buried in a half-space as shown in Figure 1. The cylinder is assumed infinite long in z direction, while the cross-section shape is arbitrary in this study. The object is illuminated by line source with Gaussian pulse located at these points denoted by Tx around the scatterer. The incident waves of TM_z polarization are generated by a home made FDTD code with fine grid to mimic the experimental data, and only reflected waves are recorded at those points denoted by Rx. In order to closely describe the shape of the cylinder for the forward scattering procedure the subgridding technique is implemented in the FDTD code.

The FDTD method solves an EM problem using the Maxwell's curl equations directly in time domain, which can be discretized to yield the following update equations of the E field for TM_z case

$$E_z^{n+1/2}\left(i+\frac{1}{2},j+\frac{1}{2}\right)=EA(m)\bullet E_z^{n-1/2}\left(i+\frac{1}{2},j+\frac{1}{2}\right) + EB(m)\bullet \left[\frac{H_y^n(i+1,j)-H_y^n(i,j)}{\Delta x} - \frac{H_x^n(i,j+1)-H_x^n(i,j)}{\Delta y} \right] \quad (1)$$

$$\text{with } EA(m)=\frac{1-\frac{\sigma(m)\Delta t}{2\varepsilon(m)}}{1+\frac{\sigma(m)\Delta t}{2\varepsilon(m)}}, \quad EB(m)=\frac{\frac{\Delta t}{\varepsilon(m)}}{1+\frac{\sigma(m)\Delta t}{2\varepsilon(m)}}$$

where $E_z^{n+1/2}\left(i+\frac{1}{2},j+\frac{1}{2}\right)$ is defined by using the Yee-cell geometry as shown in Figure 2. The expressions of the H field H_x^{n+1} and H_y^{n+1} are not given here for brevity. The boundary of

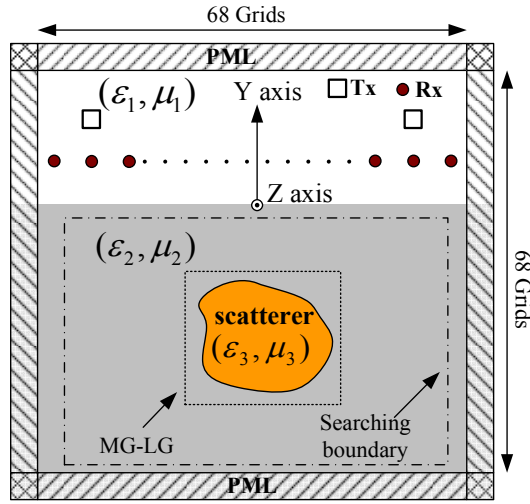


Fig. 1 Geometrical configuration for the inverse scattering

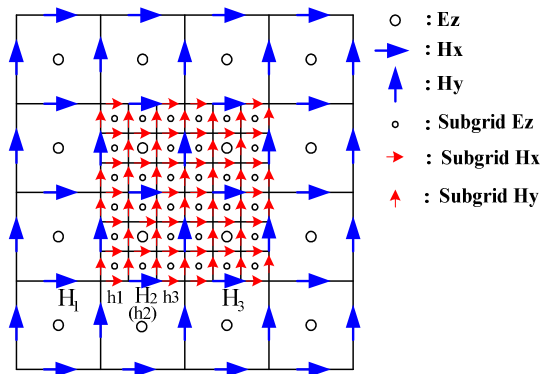


Fig. 2 The structure of the TM_z FDTD major grids and local grids for the scaling ratio (1:3) : H fields are aligned with the MG-LG boundary

the test domain is surrounded by the optimized perfect matching layer in this study.

A subgridding scheme is employed to divide the problem space into regions with different grid sizes. The grid size in coarse region is about $(\frac{1}{20} \sim \frac{1}{10} \lambda_{\max})$ as in normal FDTD, while in the fine region the grid size is scaled by an integer ratio. As an example, the Yee cells with subgridding structure are shown in Figure 2, of which the scaling ratio is 1/3. For the time domain scattering and/or inverse scattering problem, the scatterers can be assigned with the fine region such that the fine structure can be easily described. This can also avoid gridding the whole problem space using the finest resolution such that the computational resources are utilized in a more efficient way, which is quite important for the computational intensive inverse scattering problems.

In Figure 2, E and H stand for the fields on the major grids, while e and h denote those on the local grids. If the scaling ratio is set at 1:3, 1:5 and 1:7, etc, then the E and H fields coincide with e and h fields in the fine region and in the time domain as shown in Figure 2. Since the local grid size is one third of the main grid size, the time stepping interval $\Delta t'$

for the e and h fields on the local grids is also one third of that for the E and H fields on the main grids.

III. INVERSE PROBLEM AND NUMERICAL RESULTS

As shown in Figure 1, the problem space consists of three material layers divided into 68×68 grids with the grid size $\Delta x = \Delta y = 1.47$ cm. The homogeneous dielectric cylinder buried in lossless half space ($\sigma_1 = \sigma_2 = 0$). The transmitters and receivers are placed in free space above the homogeneous dielectric. The permittivities in region 1 and region 2 are characterized by $\epsilon_1 = \epsilon_0$ and $\epsilon_2 = 2.3\epsilon_0$, respectively, while the permeability μ_0 is used for each region, i.e., only non-magnetic media are concerned here. The cylindrical object is illuminated by a transmitter at two different positions, $N_t=2$, which are located at the $(-35.28\text{cm}, 14.7\text{cm})$ and $(35.28\text{cm}, 14.7\text{cm})$, respectively. The scattered E fields for each illumination are collected at the eight receivers, $M=11$, which are equally separated by 8.8cm along the distance of 7.35cm from the origin. The excitation waveform $I_z(t)$ of the transmitter is the Gaussian pulse, given by:

$$I_z(t) = \begin{cases} Ae^{-\alpha(t-\beta\Delta t)^2}, & t \leq T_w \\ 0, & t > T_w \end{cases} \quad (2)$$

where $\beta = 36$, $A = 1000$, $\Delta t = 34.685$ ps, $T_w = 2\beta\Delta t$, and

$$\alpha = \left(\frac{1}{4\beta\Delta t} \right)^2$$

The inverse problem is resolved by an optimization approach, for which the global searching scheme PSO is employed to minimize the following cost function:

$$CF = \frac{\sum_{n=1}^{N_t} \sum_{m=1}^M \sum_{t=0}^T |E_z^{\text{exp}}(n, m, t) - E_z^{\text{cal}}(n, m, t)|}{\sum_{n=1}^{N_t} \sum_{m=1}^M \sum_{t=0}^T |E_z^{\text{exp}}(n, m, t)|} \quad (3)$$

where E_z^{exp} and E_z^{cal} are experimental electric fields and the calculated electric fields, respectively. The N_t and M are the total number of the transmitters and receivers, respectively. T is the time duration of the recorded electric fields ($T=250\Delta t$ is set in this study).

The PSO is initialized with a population of random solutions which assigns a randomized velocity to each potential solution, called the particle. Thus, each particle has a position and velocity vector, and moves through the problem space. In each generation, the particle changes its velocity by its best experience, called $pbest$, and that of the best particle in the swarm, called $gbest$. Assume there are N_p particles in the swarm that is in a search space in D dimensions, the position and velocity could be determine according to the following equations:

$$v_{id}^k = w \cdot v_{id}^{k-1} + c_1 \cdot \varphi_1 \cdot (pbest_{id} - x_{id}^{k-1}) + c_2 \cdot \varphi_2 \cdot (gbest_d - x_{id}^{k-1}) \quad (4)$$

$$x_{id}^k = x_{id}^{k-1} + v_{id}^k \quad (5)$$

where v_{id}^k and x_{id}^k are the velocity and position of the i -th

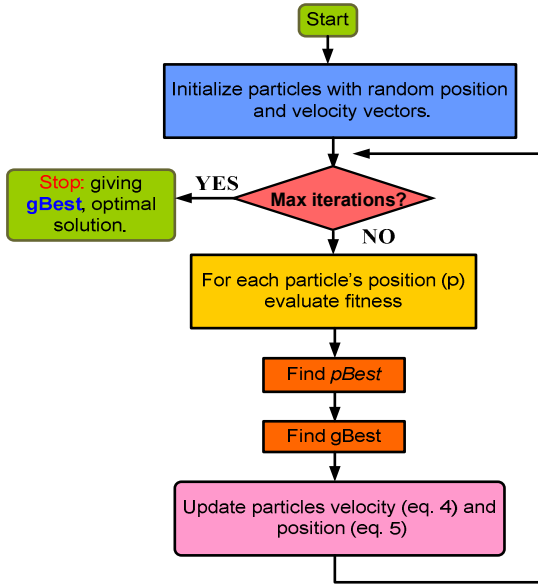


Fig. 3 Flowchart of the particle swarm optimization

particle in the d -th dimension at k -th generation, φ_1 and φ_2 are both the random number between 0 and 1, c_1 and c_2 are learning coefficients and W is the inertial weighting factor that can avoid the particle trapped into the local minimized solution. After generations, the PSO can find the best solution according to the best solution experience.

Note that in order to accurately describe the shape of the cylinder, the subgridding FDTD technique is used both in the forward scattering (1:9) and the inverse scattering (1:5) parts – but with different scaling ratios as indicated in the parentheses. For the forward scattering, the E fields generated by the FDTD with fine subgrids are used to mimic the experimental data in (3). For the inverse scattering problem, a computational technique combining with the PSO and cubic spline interpolation is reported in this paper. In order to reduce the unknowns required to describe the arbitrary cylinder, the shape function of the cylinder is expressed in terms of a closed cubic spline. As shown in Figure 3, the cubic spline consists of the polynomials of degree 3 $P_i(\theta)$, $i = 1, 2, \dots, N$, which satisfy the following smooth conditions:

$$\begin{aligned} P_i(\theta_i) &= P_{i+1}(\theta_i) = \rho_i \\ P_i'(\theta_i) &= P_{i+1}'(\theta_i) \quad i = 1, 2, \dots, N \end{aligned} \quad (6)$$

$$\begin{aligned} \text{and } P_1(\theta_0) &= P_N(\theta_N) \\ P_1'(\theta_0) &= P_N'(\theta_N) = \rho'_N \\ P_N''(\theta_N) &= P_N''(\theta_N) \end{aligned} \quad (7)$$

Through the interpolation of the cubic spline, an arbitrary smooth cylinder can be easily described through a few parameters $\rho_1, \rho_2, \dots, \rho_N$ and the slope ρ'_N . By combining the PSO and the cubic spline interpolation technique, we are able to reconstruction the microwave image efficiently.

Next, we report two numerical results of using the scheme

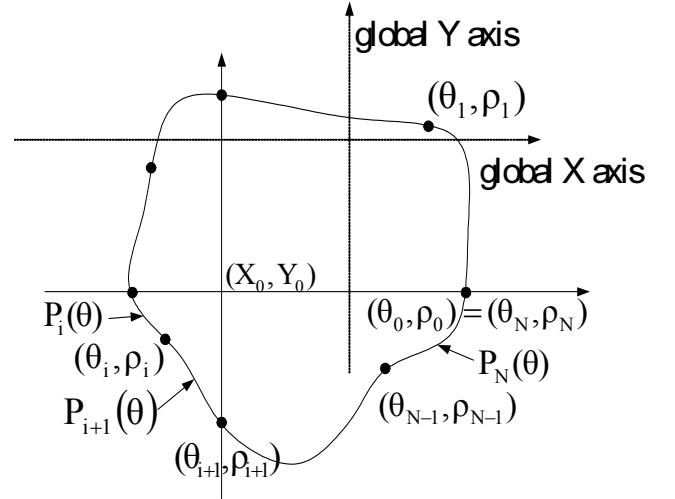


Fig. 4 A cylinder of arbitrary shape is described in terms of the cubic spline.

described above. There are twelve unknown parameters to retrieve, which include the center position (X_0, Y_0) , the ρ_i , $i = 1, 2, \dots, 8$ of the shape function and the slope ρ'_N plus the relative permittivity of the object, $\varepsilon_r = \varepsilon_3 / \varepsilon_0$. Very wide searching ranges are used for the PSO to optimize the fitness given by (8). The parameters and the corresponding searching ranges are listed follow: $-14.7\text{cm} \leq X_0 \leq 14.7\text{cm}$, $-29.4\text{cm} \leq Y_0 \leq 14.7\text{cm}$, $0\text{cm} \leq \rho_i \leq 13.2\text{cm}$, $i = 1, 2, \dots, 8$, $-1 \leq \rho'_N \leq 1$ and $1 \leq \varepsilon_r \leq 16$. The relative coefficient of the PSO are set as below: The learning coefficients, c_1 and c_2 , are both set to 2. The inertial weighting factor is set to 0.4 and the population size set to 120.

The definition of r.m.s. error (DF) of the reconstructed shape $F^{cal}(\theta)$ and the relative error (DIPE) of ε_r^{cal} with respect to the exact values

$$DF = \left\{ \frac{1}{N'} \sum_{i=1}^{N'} [F^{cal}(\theta_i) - F(\theta_i)]^2 / F^2(\theta_i) \right\}^{1/2} \quad (8)$$

$$DIPE = \left| \varepsilon_r^{cal} - \varepsilon_r \right| / \varepsilon_r \quad (9)$$

where the N' is set to 160.

The first example, a simple homogeneous dielectric cylinder is tested, of which the shape function $F(\theta)$ is chosen to be $F(\theta) = 5.88 + 2.94 \cos(\theta) + 2.94 \cos(3\theta)$ cm, and the relative permittivity of the object is $\varepsilon_r = 3.2$. The reconstructed shape function of the best population member (particle) is plotted in Figure 5 for different generation. The r.m.s. error DF is about 2.4% and DIPE= 2% in final. It is seen that the reconstruction is good.

The reconstructed result of the final example is shown in Fig. 7, where the shape is $F(\theta) = 5.88 - 1.47 \sin(3\theta)$ cm, and the relative permittivity of the object is $\varepsilon_r = 3.6$. The r.m.s. error DF is about 6.8% and DIPE=2.3%. Figure 8 shows that the relative errors of the shape and the permittivity

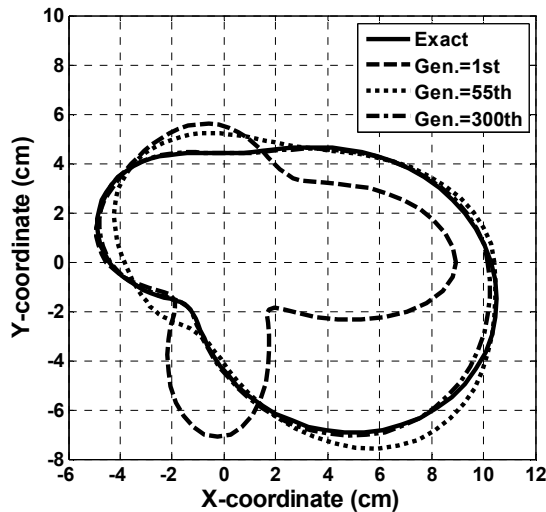


Fig. 4 The reconstructed shape of the cylinder at different generations for example 1.

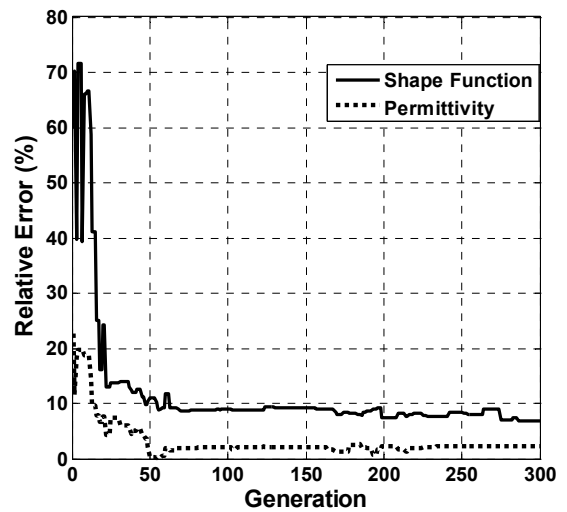


Fig. 8 Shape-function error and permittivity error at each generation of example 1.

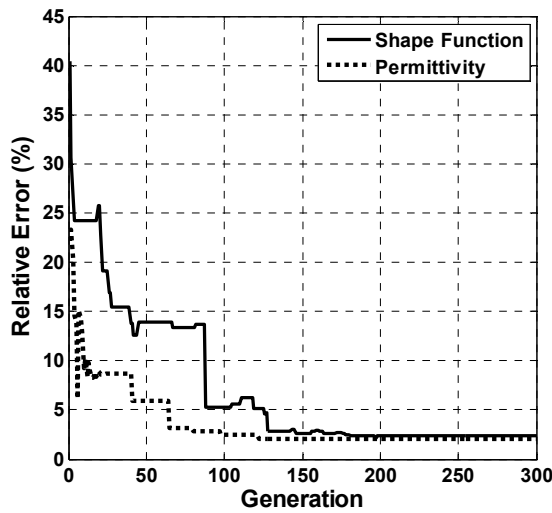


Fig. 5 Shape-function error and permittivity error at each generation of example 1.

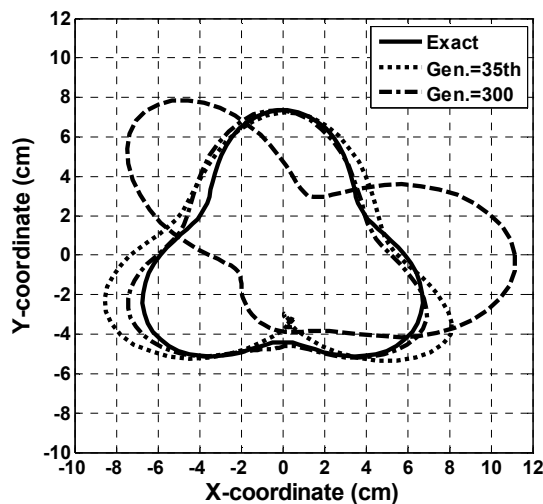


Fig. 6 The reconstructed shape of the cylinder at different generations for the final example.

decrease quickly by generations.

IV. CONCLUSIONS

In this paper, we present a study of the time domain inverse scattering of an arbitrary cross section dielectric cylinder in free space. By combining the FDTD method and the PSO, good reconstructed results are obtained by using Gaussian pulse illuminations. The subgridding scheme is employed to closely describe the shape of the cylinder for the FDTD method. The inverse problem is reformulated into an optimization one, and then the global searching scheme PSO is employed to search the parameter space. Interpolation technique through cubic spline is utilized to reduce the number of parameters needed to describe an arbitrary shape. By using the PSO, the shape, location and dielectric constant of the object can be successfully reconstructed even when the dielectric constant is fairly large.

REFERENCES

- [1] C.-C. Chiu and Y.-W. Kiang, "Microwave imaging of multiple conducting cylinders," *IEEE Trans. Antennas Prop.* vol. 40, pp. 933-941, 1992.
- [2] Y. Zhou, J. Li and H. Ling; "Shape inversion of metallic cavities using hybrid genetic algorithm combined with tabu list", *Electronics Letters.*, Vol. 39, pp. 280 -281, Feb. 2003.
- [3] V. Thomas, C. Gopakumar, J. Yohannan, A. Lonappan, G. Bindu, A.V. Praveen Kumar, V. Hamsakutty, K. T. Mathew, " A novel technique for localizing the scatterer in inverse profiling of two dimensional circularly symmetric dielectric scatterers using degree of symmetry and neural networks," *Journal of Electromagnetic Waves & Applications*, Vol. 19 No. 15, pp. 2113-2121, 2005
- [4] Eberhart, R.C. and Kennedy, J., "A New Optimizer Using Particle Swarm Theory," *Proceedings of the Sixth International Symposium on Micro Machine and Human Science*, pp. 39-43, Japan, 1995
- [5] Chevalier, M.W.; Luebbers, R.J.; Cable, V.P., "FDTD local grid with material traverse," *IEEE Trans. Antennas and Propagation*, vol.45, No.3 , March 1997.